

Nonlinear interaction between a surface acoustic wave and electron beams

Yu. M. Gal'perin, A. A. Dobrovolskiĭ, V. I. Kozub, and A. B. Sherman

I. A. Ioffe Physicotechnical Institute, Academy of Sciences USSR

(Submitted 3 May 1982)

Zh. Eksp. Teor. Fiz. **84**, 1391–1402 (April 1983)

The interaction between a surface acoustic wave and the secondary electrons produced near the surface of a piezodielectric by a primary beam of electrons is investigated theoretically and experimentally. Both linear and nonlinear (depending on the amplitude of the surface acoustic wave) regimes are studied. Special attention is paid to storage processes. Reasonable agreement is observed between theory and experiment.

PACS numbers: 79.20.Hx, 77.90.+k, 68.25.+j, 43.25.Cb

INTRODUCTION

Significant interest has developed recently in the study of the interaction of surface acoustic waves (SAW) in piezoelectric crystals with electron beams.^{1–4} The interaction considered takes place in a vacuum upon irradiation, by an electron beam, of the piezoelectric surface along which SAW is propagated. Under the action of the electron beam on the surface of the crystal, secondary electrons are emitted (with energies of the order of several electron volts), which interact with the electric fields of the SAW. As a result, the current of secondary electrons that return to the surface, turns out to be modulated. The secondary electrons incident on the surface are captured by traps present in the surface layer. This leads to the formation of a nonuniform distribution of surface charge.

As in ordinary acoustoelectric interaction in a solid, the interaction of the SAW with the secondary electrons is accompanied by its attenuation, by dispersion of the velocity of propagation, and by the generation of harmonics. In the present work we shall consider in more detail one of the most interesting aspects of the appearance of the given interaction, that is, the mechanism of acoustic storage or memory. The inhomogeneous charge distribution, which contains information about the SAW profile, can be recorded (written) on the surface of the crystal. Actually, at the instant of onset of the electron beam such a distribution ceases to change synchronously with the SAW and remains on the surface in the form of an "snapshot" of the wave profile. It is important that the charge distribution remaining on the surface can be preserved for a long time. If the surface is irradiated within the given time by the electron beam, then two acoustic waves are generated, which propagate in opposite directions, while the profiles of these waves repeat the profile of the initial SAW. The "readout" mechanism consists of the following. The secondary electrons generated by the beam tend to compensate for the inhomogeneity of the charge distribution. As a result, a nonstationary inhomogeneous electric field is produced which, as a consequence of the piezoelectric effect, generates the two opposing SAW. The indicated mechanism of acoustic memory was first studied in Ref. 1. The theory advanced in that paper was based on the analysis of the equivalent electric circuit. This circuit was assumed to be linear, which required the assumption that the potential energy of the electron in the piezoelectric field $e\varphi$ is small in compari-

son with the characteristic energy of the secondary electrons E . Thus, only a linear response could be studied within the framework of this approach. However, it is obvious that to increase the amplitude of the output signal, it is expedient to increase the intensity of the SAW and to use materials with a large electromechanical coupling constant. At the same time, the condition of applicability of the linear approximation ($e\varphi \ll E$) is violated in such materials (LiNbL₃, SiO₃ etc.) even at comparatively small intensities of the SAW—of the order of 30 mW/cm².

The aim of the present research was to investigate, both experimentally and theoretically, the interaction of the SAW with electron beams in both the linear and nonlinear regimes, paying special attention to the nonlinear situation. In part 1, along with a brief exposition of the experimental method, results are given of the experimental study of the writing and readout of SAW under the action of an electron beam that irradiates the surface of a piezoelectric crystal. In part 2, a microscopic theory of recording and reproduction is constructed in the linear and in the nonlinear regimes. It is shown that the frequency dependences of the writing efficiency differ for these two regimes. The amplitude dependence of the recorded wave saturates. The output at saturation corresponds to reaching the threshold of nonlinearity (when $e\varphi \sim E$).

1. EXPERIMENTAL RESULTS

We studied the efficiency of writing and readout of a SAW in crystalline quartz and lithium niobate. The interaction was studied in an evacuated region (vacuum of 10^{-5} – 10^{-6} Torr). The chamber with the sample, the electron beam, and a block diagram of the measurement apparatus are shown schematically in Fig. 1. The piezoelectric crystal 1, along the surface of which the wave is propagated, is placed on the metallic anode 2. On the cathode side, the working surface of the crystal is covered by a metallic screen 3 in which there is an opening which determines the dimensions of the irradiated region. A electron ribbon beam is formed by the cathode + grid unit (4, 5) constructed in the form of a Pierce gun. The current density in the electron beam and its temporal characteristics are measured by the probe 6 which is mounted over the screen. The measuring probe was a metallic surface which because of its small dimensions (2×1 mm) did not appreciably distort the current den-

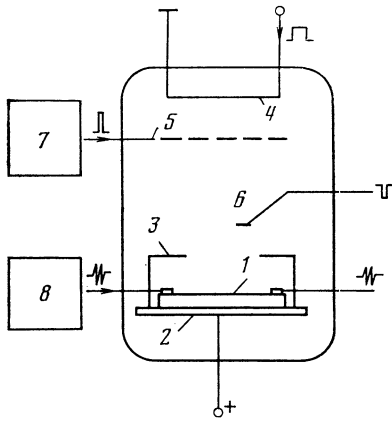


FIG. 1. Diagram of the experimental setup.

sity distribution in the electron beam. Modulation of the beam was effected by pulses fed from the generator 7 to the modulating grid 5. The pulse of the electron current in the beam has the following parameters: pulse duration t_0 from 2 to 10 ns, duration of the fronts $\Delta t_0 \sim 1$ ns. The maximum current density in the electron beam reached 2 A/cm^2 . The energy of the electron in the beam could be changed over the range from 50 to 2×10^3 eV. For writing and readout of the SAW, we used crystals of the most prevalent geometry: YX quartz and YZ lithium niobate. The SAW in these crystals was excited by an ordinary opposing-pin transducers. The working frequency range was 10–100 MHz. The maximum power of the acoustic was reached 100 W/cm .

In the writing and readout regime of the SAW, the apparatus operated in the following fashion. A current pulse heated the cathode to the working temperature (2500 C) after which the high-frequency generator 8 was triggered and excited the original SAW. Within the time necessary for propagation of the SAW to the region of interaction (of the order of $10 \mu\text{s}$), the generator 7 was triggered, which unblocked the electron beam. The beam of electrons irradiated the crystal. Upon switching off the beam a motionless electrostatic image of the SAW is produced on the surface of the crystal. Thus a record of the wave is produced. If the time of storage of the recording does not exceed 1–2 μs , the time interval is insufficient for the cathode to cool off. The system is then in a driven regime. After the lapse of time of storage, the generator 7 which produces the modulating pulse beam, is triggered again; the beam of electrons irradiates the surface of the sample on which the image of the SAW is written, and two SAW begin to propagate on both sides of the region of interaction. One SAW is similar to the initial wave while the second is its inverted analog. Writing of both the direct and the inverted waves is possible.

If the required time of storage exceeds 1–2 ms, the cathode heater block is again triggered, and the previously written SAW is now read out as a single pulse from the generator 7. The storage time amounted to several days in our experiments in the case of quartz crystals.

In correspondence with the methodology described, the efficiency of the write-readout process is determined from a comparison of the value of the output signal, obtained as a

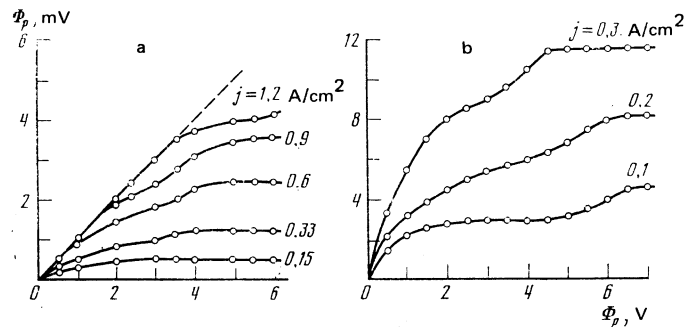


FIG. 2. Experimental dependences of the amplitude of the readout potential of the SAW on the amplitude of the initial potential of the SAW on the surface of the crystal: a) quartz, b) lithium niobate.

result of the readout, with the value of the initial signal. Such a comparison can be made for the corresponding amplitudes of the electrical potentials accompanying the wave. Just these quantities enter into the theory and with their help we can compare the results of experiment and theory.

Figure 2 shows the dependence of the amplitude of the potential of the SAW, read by the electron beam, on the amplitude of the potential of the initial SAW for quartz (a) and lithium niobate (b) at different current densities in the electron beam. The interval between the writing and readout for the substrates of both type amounted to $500 \mu\text{s}$. In each writing-readout cycle, the current density in the recording and readout beams were specified to be identical. Two characteristic regions are shown in the drawing: the region of linear growth of the amplitude of the output signal at small amplitudes of the initial SAW, and the region of saturation of this signal—at large amplitudes. Both for quartz and for lithium niobate the transition from the linear region to the nonlinear takes place at an electric potential of the order of several volts in the initial SAW.

The following two circumstances must also be noted. For sufficiently high currents in the electron beam, as follows from Fig. 2, the amplitude of the read-out signal does not depend on the current density. The ratio of the amplitudes of the readout and initial SAW's in this region is maximal and constant. For YX quartz, it is equal to 10^{-3} . The other important circumstance is that the linear region expands with increase of the current in the electron beam. For lithium niobate, similar dependences are observed; however, no saturation of the initial memory signal as a function of the current density in the electron beam is observed up to currents of the order of hundreds of mA/cm^2 . The writing efficiency in the case of a current of 300 mA/cm is 40 dB.

The dependences set forth above were obtained upon writing and readout of the SAW by current pulses with duration $t_0 = 10$ ns. As experiment shows, the amplitude of the readout signal for the case of small currents depends on the duration of the current pulse. This dependence is shown in Fig. 3. The period of oscillation of the readout signal was identical with the period of the SAW, while the damping of the oscillations increases with increase of the current density in the electron beam, so that at sufficiently high current densities the stationary amplitude of the readout signal is

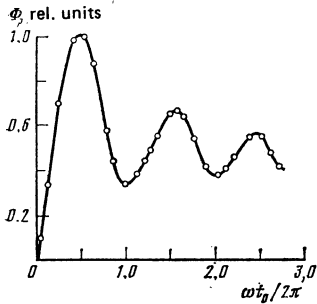


FIG. 3. Dependence of the amplitude of the readout signal on the pulse duration of the electron beam. The maximum value of the current density is 50 mA/cm^2 .

reached at pulse durations t_0 that are relatively short in comparison with the period of the wave, $2\pi/\omega$. The maximum values of the damped sinusoid in Fig. 3 correspond to pulse durations $2\pi/n\omega$, where $n = 1, 2, 3, \dots$. It is obvious that the condition $\omega\Delta t_0 \ll 1$ should be satisfied for writing and readout. Since the modulating pulse that we used had a rise time $\Delta t_0 \approx 1 \text{ ns}$, the condition given above is completely satisfied up to frequencies of the order of 100 MHz. Figure 4 shows the frequency dependence of the current density in the electron beam that is necessary for obtaining the given amplitude of the readout signal. It follows from the drawing that this current density increases quadratically with increase in the frequency of the SAW. The character of this dependence is preserved for both the linear and the nonlinear regimes.

It should be noted that the values of the readout signals of the SAW depend on the geometry of the electric field near the surface of the crystal. Thus, for example, the presence on the surface of a screen grid, located above the potential anode, significantly lowers the electron-beam current density necessary for obtaining the readout signal of specified amplitude (the data used in the graphs were obtained without the grid).

2. THEORY

In order to avoid unimportant complications associated with the analysis of the nonuniform distribution of large-scale static fields due to the external electrons, we assume

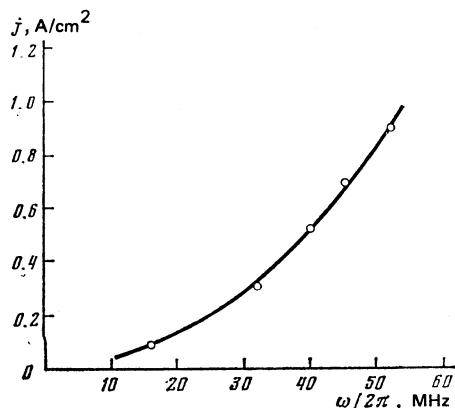


FIG. 4. Dependence of the current density in the electron beam on the frequency of the SAW.

that a screen grid connected to the anode is situated above the sample, close to its surface (but at a distance much greater than the wavelength). Secondary electrons with characteristic energy E , knocked out by the primary beam, in part shoot through this grid, and in part are turned back to the surface of the sample. Here the charge of the surface and its potential are determined by the balance of flows of primary and secondary electrons. It is easy to see from an analysis of this balance that the potential of the surface relative to the anode is of the order of the characteristic energy of the secondary electrons E .

Let a SAW propagate along the surface of the sample. As a consequence of the piezoelectric interaction an alternating electric field is generated in the vacuum over the surface, with a potential

$$\varphi_p = \Phi_p \exp(-qz + iqx - i\omega t) + \text{c.c.} \quad (1)$$

Here the z axis is directed along the normal to the surface, $\Phi_p \sim 4\pi\beta u_{ik}^0/\epsilon q$, β is the characteristic value of the component of the tensor of piezoelectric coefficients, u_{ik}^0 is the amplitude of the strain tensor, ϵ is the permittivity of the sample. This field acts on the secondary electrons which, becoming redistributed in space, screen the primary potential. Thus, the problem of the resultant field on the surface must be solved in self-consistent fashion. For this purpose, we calculate the surface charge density of the secondary electrons returning to the surface and "sticking" to it. The time derivative of this quantity is equal to the normal component j_z of the current density of the secondary electrons, which is determined by the expression

$$j_z(x)|_{z=0} = e \int (d\mathbf{p}) v_z f(\mathbf{v}; x; z=0), \quad (2)$$

where \mathbf{v} is the velocity of the electrons, $f(\mathbf{v}, x, z)$ is the electron distribution function, and $(d\mathbf{p})$ is an element of phase space. Under good vacuum conditions, the electrons move ballistically over the surface. In this case, according to Liouville's theorem, the distribution function is constant along the trajectory, and is determined by the equation of motion. In this connection, it is convenient to introduce the new variables v_0 and x_0 , which characterize the velocity and the x coordinate of the electron at the initial point of a trajectory that terminates on the surface at the point x . Thus,

$$j_z = e \int (d\mathbf{p}_0) v_z(\mathbf{v}_0, x_0) g(\mathbf{v}_0)/v_{z0}. \quad (3)$$

Here $v_x(\mathbf{v}_0, x_0)$ is the velocity, at the point x , of an electron knocked out of the surface at the point x_0 at an initial velocity \mathbf{v}_0 , $g(\mathbf{v})$ is the generating function of the secondary electrons knocked out of the surface. The quantity $g(\mathbf{v}_0)$ in (3) is specified and is determined by the characteristics of the primary beam and the material of the sample. We shall assume it to be constant over the surface. For the determination of $v_z(\mathbf{v}_0, x_0)$, it is necessary to solve the equation of motion of the electron in the given potential.

We begin our consideration with the linear case, in which the condition

$$e\varphi \ll E \quad (4)$$

is satisfied. In this case the contribution Δv_z to the velocity of

the electron, due to the presence of the piezoelectric field, is defined by the integral

$$\Delta v_z = -\frac{e}{m} \int dt \frac{\partial \varphi(x, t)}{\partial z}, \quad (5)$$

calculated along the unperturbed trajectory of the electron. Since the characteristic dimension of the trajectory in the z direction is much greater than the wavelength q^{-1} (in our geometry this dimension is of the order of the distance to the screen grid), we can neglect the curvature of the trajectory in this integral, since the potential φ is not small only in a layer of thickness $\sim q^{-1}$. Taking this into account and substituting (5) in (3), we obtain the following expression for the contribution to the z -component of the current:

$$\Delta j_z = e\varphi(x) \int (d\mathbf{p}) g(v_0) / m (v_{x0}^2 + v_{z0}^2). \quad (6)$$

In order of magnitude $\Delta j_z \approx (\nu - 1) J_0 e \varphi(x) / 2E$, where J_0 is the current density in the primary beam. The factor $(\nu - 1)$ is associated with the fact that the redistribution of the current is assured only by the secondary electrons returning to the surface of the sample. Since the sound velocity is much smaller than the characteristic velocity of the electron, we can use here the equation of electrostatics. Starting out from the expression for the potential of a charged filament lying on the vacuum-dielectric interface (see Ref. 5), we obtain the following expression for the x component of the field created by the surface charge

$$\begin{aligned} \tilde{\mathcal{E}}_x &= -\frac{\partial \tilde{\varphi}}{\partial x} = -4e(1+\varepsilon)^{-1} \left(\frac{\partial}{\partial x} \int_{-\infty}^{\infty} dx' n(x) \ln|x-x'| \right) \\ &= 4\pi n_0 e (1+\varepsilon)^{-1} i \exp(iqx). \end{aligned} \quad (7)$$

Here $en(x) = en_0 e^{iqx}$ is the surface charge density. Differentiating (7) with respect to the time, taking into account the fact that $en(x) = j_x$, and adding the potential of the unrenormalized piezoelectric field, we obtain the following equation for the total electric potential on the surface:¹⁾

$$\varphi(x, t) + \frac{1}{\tau_J} f(t) \varphi(x, t) = -\psi_p(x, t). \quad (8)$$

Here

$$\tau_J^{-1} = 2\pi(\nu-1)eJ_0/q(1+\varepsilon)E; \quad (9)$$

f is a function describing the turning-on of the electron beam.

We now consider the processes of writing and readout. Let $f(t) = \theta(t)$, where $\theta(t)$ is the Heaviside function. The solution of Eq. (8) is naturally written in the form

$$\varphi(x, t) = \varphi_0(t) e^{iqx} + \text{c.c.}$$

with the initial conditions $\varphi_0|_{t=0} = \varphi_p|_{t=0}$. For the function $\varphi_0(t)$ we obtain the following expression from (8):

$$\varphi_0(t) = \Phi_p \frac{1}{(1-i\omega\tau_J)} \left[\exp\left(i\omega - \frac{1}{\tau_J}\right) t - i\omega\tau_J \right]. \quad (10)$$

Subtracting the unrenormalized piezoelectric potential φ_p from (10), we obtain the expression for the potential of the stuck-on charge—the “memory signal” φ_s . At the instant t_0 corresponding to turning-on of the initial beam, this expres-

sion is equal to

$$\varphi_s = \Phi_p (1-i\omega\tau_J)^{-1} \left[\exp\left(i\omega - \frac{1}{\tau_J}\right) t_0 - 1 \right]. \quad (11)$$

Thus, as a result of the recording process, a nonuniform potential distribution $\varphi_s e^{iqx} + \text{c.c.}$ arises which produces as a consequence of the piezoelectric interaction a nonuniform static strain equal to $u_s = \beta\varphi_s/c$, (as follows from the equations of elasticity theory); here c is the corresponding component of the elastic-moduli tensor.

We now proceed to the readout process. At the time $t = 0$, let the electron beam with a switch-on function $\theta(t)$ begin to act on the plate with the recorded signal. For a description of the readout process, it is necessary to solve a system consisting of the equations of elasticity theory and Eq. (8). We assume a piezoelectric-interaction constant $\chi = 4\pi\beta^2/\varepsilon c \ll 1$. In this case, we can neglect the right side of Eq. (8) and solve it with the initial condition $\varphi|_{t=0} = \varphi_s$. The solution has the form

$$\varphi(t) = \varphi_{s0} \exp(iqx - t/\tau_J) + \text{c.c.} \quad (12)$$

Representing the displacement $u(x, t)$ in the form $u_0(t) \exp(iqx)$, we obtain the following equation for $u_0(t)$:

$$d^2 u_0 / dt^2 = -\omega^2 u_0 + (\beta q^2 \varphi_{s0} / \rho) \exp(-t/\tau_J), \quad \omega = wq, \quad (13)$$

w is the speed of sound, ρ is the density of the crystal. Solving this equation with the initial condition $u_0(0) = u_s$, we obtain the following expression for the displacement $u(x, t)$:

$$\begin{aligned} u(x, t) &= (u_s/2) [1 + (\omega\tau_J)^2]^{-1/2} \\ &\times \{ \cos(qx - \omega t + \alpha) + \cos(qx + \omega t - \alpha) + 2(\omega\tau_J)^2 [1 + (\omega\tau_J)^2]^{-1/2} \\ &\times \exp(-t/\tau_J) \cos qx \}, \quad \alpha = \arctg(\omega\tau_J). \end{aligned} \quad (14)$$

The first two terms in the curly brackets in (14) describe two acoustic waves propagating in opposite directions; the last term describes the “erasing” of the memory signal u_s in the readout process. Thus the recording-readout efficiency K , which we shall define as the ratio of the intensities of the readout and initial SAW's, is equal to

$$K = \left(\frac{u_r}{u_w} \right)^2 = \frac{\chi^2 [1 + \exp(-2t_0/\tau_r) - 2 \exp(-t_0/\tau_w) \cos \omega t_0]^2}{4 (1 + \omega^2 \tau_w^2) (1 + \omega^2 \tau_r^2)}. \quad (15)$$

Here the indices w and r correspond to processes of writing and readout, the time τ in the case of writing and reading can generally be different, since the writing and readout can occur at different currents. In particular, it is seen from (14) that in the case of readout, the written signal is erased with characteristic speed τ_r^{-1} ; therefore, if there is need of multiple readout, the regime $J_r < J_w$ is preferable.

We now proceed to the consideration of the nonlinear regime. We shall limit ourselves here to an approximate treatment, which allows us to analyze the physical picture and the basic laws. We shall assume that the condition of strong nonlinearity is satisfied, i.e., $e\varphi \gg E_k|_{z=0}$, where $E_k|_{z=0}$ is the kinetic energy of the secondary electrons at the moment of their appearance on the surface. The total energy of the secondary electrons

$$E = E_k + e\varphi(r, t)$$

is conserved along the trajectory. We note that the potential

φ consists of two parts, which depend differently on the coordinates: the "fast" $\tilde{\varphi}$, which changes over characteristic distances q^{-1} , and the "slow" $\bar{\varphi}$ which changes over distances of the order of the distance l_e to the nearest electrode. The second part is due to the uniform charging of the surface by the electrons and guarantees a balance of the currents. In the linear regime, its value is of the order of the characteristic energy E_k of the secondary electrons; the effect of sound on this part of the potential can be neglected. However, we shall see that in the nonlinear regime this is generally not the case. Two contributions to the force acting on the electron can be connected with the two components mentioned: the slow $\tilde{f} = e\bar{\varphi}/l_e$ acting along the z axis, and the fast $\tilde{f} \approx -e\nabla\tilde{\varphi}$, localized near the surface.

To begin with, in the consideration of the electron trajectories, we shall neglect the contribution of \tilde{f} (as is easy to see, $\tilde{f} \ll \tilde{f}$ in a strongly nonlinear regime). We note that if the force f is sufficiently large, then the electron produced at a point where $\tilde{f}_z < 0$ cannot move from the surface (the characteristic size of its trajectory in the z direction $E_k|_{z=0}/qe\varphi$). By virtue of this fact, such electrons (produced in regions of potential wells) do not make a contribution to the redistribution current. The change in the surface charge in these regions is thus due to the contribution of the primary beam, and also to such electrons that arrive from other points of the surface and from greater distances ($z \gg q^{-1}$). The current density corresponding to the contribution of these electrons is denoted by $J_+(x)$. On the other hand, if $f_z > 0$ ("humps"), then all the secondary electrons depart from the surface. The trajectories of such electrons can be different; they can terminate on the nearest electrode, in a distant region, and also in nearby potential wells. The density of the current from the surface in these regions is of the order of νJ_0 ; the current density on the surface includes the contribution of the primary beam J_0 . And also, in principle, the contribution of electrons arriving from the distant region, i.e., those produced on other humps. In sum, the total current density j_z can be written down in the form

$$j_z = \begin{cases} J_0 - \nu J_0 + J_+(x), & e\bar{\varphi} > 0, \\ J_0 + J_+(x), & e\bar{\varphi} < 0. \end{cases} \quad (16)$$

For the determination of the redistribution current density $J_+(x)$, it would be necessary in the case of a given potential relief to solve a rather complicated numerical problem. Here we shall not do this, but will assume it to be given. It is clear that the current J_+ is proportional to J_0 and has the same order of magnitude (if $\nu \sim 1$). Therefore, we put $J_+(x) = J_0 \zeta(x)$, where $\zeta(x)$ is determined from the potential relief. (The quantity ζ generally depends also on $\bar{\varphi}$ because of the contribution of electrons returning from the distant region.)

We consider the surface-charge balance. Using the estimate set down above for J_+ , we obtain the following equation for the slowly changing part of the electric field $\bar{\zeta}$ in space:

$$\bar{\zeta}_z = (J_0 l_e / Cl_e) [1 + \zeta(x) - \nu \theta(-\bar{\varphi})], \quad (17)$$

where C is the specific surface capacity once (normalized over the width of the interaction region and thus dimension-

less), l_e is the length of the interaction region in x direction. For the fast part of the electric field, we have, with consideration of (7),

$$\bar{\zeta}_x = -4\pi J_0 (1 + \varepsilon)^{-1} \int_{-\infty}^{\infty} dx' (x - x')^{-1} \{ \zeta(x') - \nu \theta(-\bar{\varphi}(x')) - [\zeta(x') - \nu \theta(-\bar{\varphi}(x'))] \} + \dot{\zeta}_{px}. \quad (18)$$

The initial conditions for (17) and (18) are

$$\bar{\zeta}|_{t=0} = 0, \quad \dot{\zeta}_x|_{t=0} = \dot{\zeta}_{px}.$$

We discuss the qualitative picture. As was seen, this redistribution changes in space "in antiphase" with the potential, namely, more electrons land in the wells than in the humps. Therefore, as also in the linear case, the electrons fill the potential wells and decrease the potential. In the course of this process, the redistribution current $\tilde{j} \sim j_z - \tilde{j}_z \sim J_0$ until $\varphi \lesssim \varphi_p$ or, at least until $e\bar{\varphi} \gtrsim E_k$. At this time, $\varphi \lesssim 4\pi J_0 / q(1 + \varepsilon)$. If the potential φ_p were stationary, it would be completely shielded within a time of the order

$$\tau_\varphi = q\Phi_p(1 + \varepsilon) / 4\pi J_0 = \tau_J (e\Phi_p / E_k). \quad (19)$$

Since we assume that $e\varphi_p \gg E_k$, the inequality $\tau_\varphi \gg \tau_J$ holds. In this discussion, we have assumed the profile of the acoustic wave to be static. In fact, it varies at a frequency ω , and if $\omega\tau_\varphi \gg 1$, the screening is ineffective—the electrons do not have time to fill the well. Actually, the right side of (18) changes sign within a half-period. Therefore, the characteristic estimate for the potential of the surface charge is determined by the integral of the right side of (18) over a time equal to one half the period of the SAW. Thus, if $\omega\tau_\varphi \gg 1$, the ratio of the surface charge potential to the unrenormalized potential is of the order of $(\omega\tau_\varphi)^{-1}$ and the total potential almost reaches the piezopotential Φ_p . We note that in this case the total potential has practically a sinusoidal shape, whereas the form of the potential of the surface charge is far from sinusoidal. It is also important to note that the characteristic amplitude of this potential is estimated at $E_k / \omega\tau_J$, i.e., it does not depend on Φ_p —the memory signal reaches saturation. In these discussions we have assumed that the pulse duration of the primary current t_0 is much greater than ω^{-1} . In the opposite case, the characteristic parameter is the quantity t_0 / τ_φ (if $t_0 \ll \tau_\varphi$).

This is the situation upon satisfaction of the condition $\omega\tau_J \gg 1$ (when the condition of strong nonlinearity automatically leads to the inequality $\omega\tau_\varphi \gg 1$). If $\omega\tau_J \ll 1$, then the situation is more complicated. For its analysis, we write down the equation (18) in the form

$$\dot{\bar{\zeta}} = \frac{E_k}{\tau_J} \mathcal{F}(E, \bar{\varphi}). \quad (20)$$

In the case of very high sound intensities, when $e\bar{\varphi} \gtrsim E$, the functional is $\mathcal{F} \sim 1$ and corresponds to saturation—all the secondary electrons are expended in filling the potential wells. If $e\bar{\varphi} \ll E_k$, then the functional is $\mathcal{F} \sim e\bar{\varphi} / E_k$, as is clear from what has been said above. Using (20), it is easy to see that in the case

$$\omega\tau_\varphi = \omega\tau_J e\Phi_p / E_k \gg 1$$

the situation is similar to that described above—the total potential almost equal to the unrenormalized one, while the potential of the stuck charges becomes saturated. If the intensity is so low that the condition

$$\omega\tau_\varphi = \omega\tau_J e\Phi_p/E_k \ll 1.$$

is satisfied, we find ourselves under conditions of applicability of linear theory. Actually, under such conditions, the product $\omega\tau_J\Phi_p$ is none other than the resulting potential acting on the electrons, so that the condition $\omega\tau_\varphi \ll 1$ is equivalent to the condition of applicability of the linear theory. The behavior of the amplitude of the effective potential φ is more complicated in its dependence on the amplitude of the unrenormalized potential φ_p in the case $\Phi_p \sim E_k e\omega\tau_J$. With these amplitudes, a transition takes place from the linear screening (when $\bar{\varphi} \sim \omega\tau_J\Phi_p \ll \Phi_p$) to the nonlinear (when $\bar{\varphi} \sim \Phi_p$). In such a transition, the potential of the stuck charges goes into saturation, while its profile becomes essentially nonsinusoidal.

We not return to the discussion of the slow part of the potential connected with the uniformly charged surface. The behavior of this potential in the nonlinear regime depends essentially on the value of the secondary-emission coefficient ν . For illustration, we assume that $\xi = 0$ and $\bar{\varphi} \ll \varphi$. It then follows from (17) that $\bar{\mathcal{E}}$ vanishes if $\nu = 2$. If $\nu > 2$, then the surface is positively charged, if $\nu < 2$, it is negatively charged. The critical value $\nu = 2$ reflects the fact that the electrons can depart from only half the surface—from the humps. Actually, $\xi \neq 0$; therefore $\nu_c > 2$, as is easily seen.

We begin with the case $\omega\tau_\varphi \gg 1$. Returning to Eq. (17) and substituting for $\bar{\varphi}$ in it the potential φ_p , it is easy to establish the fact that $\bar{\mathcal{E}} \neq 0$. Therefore, in correspondence with this equation, the modulus of the potential of the sample would be changed in time to infinity. This is connected with the fact that in the derivation of (17), we have assumed $\bar{\varphi} = 0$, which is valid only at the initial instant and is suitable for the estimate of the derivative at this moment. But the established value of the mean potential can be estimated from a consideration of the balance of the total charge. At $\nu > \nu_c$, when the surface is positively charged, the charging continues until the total current at the surface vanishes, i.e., until the number of electrons returning to the surface becomes sufficiently large and compensates for the outflow. Since we have assumed that $e\varphi_p \gg E_k|_{z=0}$, the kinetic energy of an electron leaving the hump is $\sim e\Phi_p$ far from the surface. Thus, the return is effective at $\bar{\varphi} \gtrsim \Phi_{p0}$. This is in fact the estimated mean potential of the surface. It is seen that this value is achieved within a time of the order of

$$\tau_{c1} \approx (I_0 J_0 / C \Phi_p)^{-1} \ll \tau_\varphi.$$

In this case, the mean field $\bar{\mathcal{E}} \sim \Phi_p/l_e$, which is significantly less than the field in the wave $\sim q\Phi_p$. If $\nu < \nu_c$ and the surface is negatively charged, then the return current from the distant regions generally does not arise—those electrons which penetrate into the distant regions are incident on the grid. Therefore the charge balance is determined by the value of the mean field in the subsurface layer. If this field is less than the field of the wave (more precisely, its z component), then all the dynamics in the subsurface layer are determined

by the field of the wave and the balance is not assured. Balance can be achieved only in the case of a mean field of the order of the field in the wave, i.e., at $q\Phi_p \sim \bar{\varphi}/l_e$. Thus, $\bar{\varphi} \sim \varphi_p (q l_e \gg \varphi_p)$. Correspondingly, the time of charging the surface is $\tau_{c2} \sim (I_0 J_0 / C \Phi_p q l_e)^{-1} \sim \tau_{c1} q l_e \sim \tau_\varphi$. If the time of action of the beam t_0 is less than the characteristic time of charging, then the surface is charged to a potential that is small to the extent that the ratio $(t_0/\tau)\bar{\varphi}_{\text{lim}}$ is small. If, however, $\omega\tau_\varphi \ll 1$ then, as we have seen, the situation is close to linear. The change in the mean potential is then smaller and has the order of $\sim E_k (e\Phi_p/E_k)^2$.

In all the succeeding discussion, we shall not take into account the mean charging of the surface (although in the case of a negative charging of the surface, as we have seen, the latter can acquire a rather large potential). The fact is that all the estimates given above for the alternating field remain in force, since in the estimate of the time τ_φ for the variable field remain in force, inasmuch as we have used in the estimate of the time τ_φ only the boundedness of the functional \mathcal{F} . However, we note that the large negative potential acquired by the surface in the strongly nonlinear regime can affect the energy of the primary electrons reaching the surface and, by the same token, affect the coefficient of secondary emission.

The estimates given above allow us to obtain the basic relations characterizing the efficiency of the memory in the nonlinear regime. The amplitude of the sticking charge characterizes the memory signal. The readout process can be analyzed with the help of the equations of elasticity theory, with account of the smallness of the electromechanical coupling constant (as is done in the linear regime). Here two variants are possible. If the writing signal is small ($e\varphi_s < E_k$), then the readout process is generally linear. It is important to keep the following in mind here. The writing signal (the profile of the surface charge) does not duplicate with perfect accuracy the initial wave, as a consequence of the nonlinearity of the process, but contains a number of higher harmonics. However, in the case of linear readout, as calculation shows, the higher harmonics of the readout wave are damped in comparison with the harmonics of the surface potential by a factor of n^2 in amplitude, where n is the number of the harmonic. This fact is a consequence of the significant dependence of the time τ_J on the frequency. If the potential of the sticking charges is large, then the readout is also nonlinear. Here the readout signal possesses a richer harmonic content in comparison with the profile of the surface potential. The amplitude of the readout signal is determined by the same estimates as in the linear theory, with the substitution $\tau_J \rightarrow \tau_\varphi$. It then follows that if our aim is to reproduce the given wave more accurately, we should operate in every case in the regime of linear readout (we are speaking here of the accuracy of reproduction of the high-frequency carrier of the acoustic wave and not of its envelope).

In conclusion to this section, we shall give a resume of the estimates of the efficiency of the write-readout process in the nonlinear regime under satisfaction of conditions that are typical for the experiment: $t_0 \gg \omega^{-1}$, $\omega\tau_J \gg 1$. As we have seen, the parameter of nonlinearity for the set of such pro-

cesses is actually the quantity $\omega\tau_{\varphi w} = \omega\tau_{Jw}e\Phi_p/E_k$, and the nonlinearity is significant when it reaches unity. In this situation, two variants are possible:

1) $\omega\tau_{Jw} \gg 1$. The writing is nonlinear, the readout linear:

$$K = \left(\frac{\chi}{\omega^2 \tau_{\varphi w} \tau_{Jr}} \right)^2 \approx \left(\chi \frac{E_k}{\omega^2 \tau_{Jw} \tau_{Jr} e \Phi_p} \right)^2 \approx \frac{\omega^{-8}}{S}. \quad (21)$$

The surface potential relief here is nonharmonic, while the readout wave is close to harmonic.

2) $\omega\tau_{Jr} \ll 1$. The writing and readout processes are nonlinear:

$$K = (\chi E_k / \omega \tau_{Jr} e \Phi_p)^2 \approx \omega^{-4} / S. \quad (22)$$

The readout signal is rich in harmonics.

We note that according to our theory, in the equality of the writing and readout currents both in the linear and nonlinear regimes, the value of the current necessary for realization of the given efficiency of the write-readout process changes in proportion to the square of the frequency.

3. DISCUSSION OF RESULTS

We now compare the experimental and theoretical results. As is seen from Fig. 2, two characteristic regions are clearly differentiated by experiment; in these the dependences $\varphi(\varphi_p)$ are different. At small amplitudes, the dependence is linear, which agrees with Eqs. (11) and (15); at large amplitudes, φ_r reaches saturation, which agrees with the conclusions of the nonlinear theory. Here, as is seen from the drawing, the value of the potential of the wave corresponding to the transition from linear dependence to nonlinear corresponds in order of magnitude to the most probable value of the energy of the secondary electrons E . The fact that the value of the readout signal ceases (at sufficiently large currents) to depend on J_0 in the linear region with increase in the current density agrees with theory. Actually, according to (15), the quantity K ceases to depend on τ_J at $\omega\tau_J \ll 1$ and $\tau_J \sim J_0$. In this region, the write-readout efficiency, determined experimentally, is in agreement with theory. At $\omega\tau_J \gg 1$, theory predicts a quadratic dependence of the amplitude of the readout signal on J_0 (in the equality of the writing and readout currents), see Eq. (15). Unfortunately, the amplitude of the readout signal in this regime is not sufficiently large to be measured reliably and to allow us to establish its dependence on the current with certainty. Within the limits of accuracy of the experiment, our results, which follow from Fig. 2, do not contradict the quadratic dependence. The $K(t_0)$ dependence which follows from (15) should have an oscillatory character. This fact is in agreement with the results of experiment (Fig. 2). In addition, the locations of

the maxima are identical. Unfortunately, however, it is not possible to carry out a numerical comparison of Eq. (15) with the results represented in Fig. 3, since the data shown in Fig. 3 refer to the nonlinear regime ($e\varphi \gtrsim E_k$). It is difficult to obtain the oscillatory dependence of $K(t_0)$ in the linear regime; the region of oscillations arises at $\omega\tau_J \gg 1$, and here, as we have seen, the readout signal is very small.

We now proceed to the discussion of the nonlinear regime. First of all, we note that the threshold of nonlinearity $e\varphi \sim E_k$ itself depends on the current density, since the screening of the unrenormalized potential Φ_p depends on J_0 and consequently also the amplitude of φ at a given intensity of the initial signal [see (11)]. As a result, the nonlinearity threshold shifts toward higher intensities of the SAW with increase in the current (Fig. 2). In the essentially nonlinear region (saturation) the dependence of the amplitude of the readout signal on J_0 , which follows from Fig. 2, is quadratic at small J_0 and linear at large J_0 . These dependences agree with Eqs. (21) and (22). Finally, Fig. 4 shows that the only nondimensional parameter characterizing the behavior of the considered system and dependent on the current J_0 is the product $\omega\tau_J$. Actually, the constancy of this parameter corresponds to the dependence $J \sim \omega^2$, which agrees with Fig. 4. It is important that such a dependence also takes place in the linear regime, which is due to the proportionality between $\omega\tau_J$ and the nonlinearity parameter $\omega\tau_\varphi$.

Thus, the experimentally observed dependences agree with the theoretical predictions.

¹We do not take into account the space charge of the secondary electrons located above the surface of the sample. It is easy to show that their contribution is negligible in comparison with the contribution of the surface charge, and this is the essential difference of our theory from the theory of layered piezoelectric-semiconductor systems.

¹A. G. Bert, B. Epsztajn and G. Kantorowicz, Appl. Phys. Lett. **21**, 50 (1972). Rev. Techn. Thomson-CSF **8**, 503 (1976). IEEE Trans. on Microwave Theory and Techniques MTT-**21**, 255 (1973).

²A. B. Sherman, E. V. Balashova, A. A. Dobrovolskiĭ, V. V. Lemanov and L. I. Trusov, Pis'ma Zh. Tekhn. Fiz. **1**, 1108 (1975) [Sov. Phys. Tech. Phys. Lett. **1**, 474 (1975)]. E. V. Balashova, A. A. Dobrovolskiĭ, V. V. Lemanov, A. B. Sherman, Yu. M. Gal'perin and V. I. Kozub, Fiz. Tverd. Tela **21**, 3086 (1979) [Sov. Phys. Solids State **21**, 1775 (1979)].

³G. A. Bernashevskii, N. S. Voronov, Yu. V. Gulyaev, I. M. Kotelyamskiĭ, N. A. Ovchinnikov, Z. S. Chernov and A. E. Shabel'nikova, Pis'ma Zh. Tekh. Fiz. **7**, 780 (1981) [Sov. Phys. Tech. Phys. Lett. **7**, 335 (1981)].

⁴V. I. Voroshen', and N. M. Chirkin, Radiotekhnika i elektronika **26**, 2234 (1981).

⁵L. D. Landau and E. M. Lifshitz, Élektrodinamika sploshnykh sred (Electrodynamics of Continuous Media) Moscow, Fizmatgiz, 1959, p. 60. English translation, Pergamon Press, Oxford, 1960).

Translated by R. T. Beyer